The effects of monetary policy on macroeconomic downside risk: state-dependence matters*

Giovanni Barci †

May 2024

Abstract

I study the causal relationship between monetary policy and macroeconomic downside risk, focusing on the analysis of structural asymmetries across economic states (i.e., recession and expansion). I define downside risk indicators as linear combinations of relevant quantiles of the conditional expected density of output growth and recover state-dependent (linear combination of) quantile IRFs adopting a novel econometric framework that combines SVAR and quantile regressions, both adapted to accommodate smooth-transition parameters. I find that the magnitude of the reduction in downside risk following a monetary easing during recessions is about four times higher than its specular increase in the aftermaths of a monetary tightening during booms. The conclusion holds also when considering monetary contractions during highly-leveraged expansions. Finally, financial conditions seem to play a key role in transmitting the monetary policy shock to downside risk asymmetrically across economic states.

Keywords: Downside risk; monetary policy; state-dependence; SVAR; quantile regression

JEL codes: C32, C53, E32

*I am grateful to Luca Gambetti for his guidance. I would also like to thank Fabio Bagliano, Davide Debortoli, Francesco Furlanetto, Jordi Galì, Francesca Loria, Giovanna Nicodano, Federico Ravenna and the participants of various conferences and seminars for helpful comments and discussions.

†Collegio Carlo Alberto & University of Turin (giovanni.barci@carloalberto.org)

1 Introduction

One of the key functions of central banks is to overview risk. In recent years, much attention of monetary policy-makers has been devoted to downside risks to the economy (FED (2008), BoE (2020), ECB (2024)). Whereas there has been an obvious focus on the role of macro-prudential operations in shaping risk (Chavleishvili et al. (2021)), the relation between this and monetary policy still remains relatively unexplored. The reason is that the monetary policy-downside risk connection is more nuanced. However, it may be particularly relevant. Specifically, despite monetary interventions not being directly targeted at managing risk, they are likely to have important effects in shaping it via their impact on business cycle fluctuations and inflation patterns. The recent evidence put forward in Forni et al. (2023) and Loria et al. (2022) precisely points in this direction. Nonetheless, both these works carry a limitation, namely they focus only on the average effects (across time) of monetary policy on downside risk, which may be misleading to monetary policy-makers. The reason is that, given the business cycle-smoothing function of monetary policy, significant policy interventions are naturally associated to periods in which economic growth considerably deviates from its mean, and it may well be the case that the response of downside risk to monetary policy differs based on the specific phase of the business cycle (i.e., expansion/recession). This paper precisely aims to investigate whether this is the case. Specifically, I study what are the effects on downside risk of an unexpected monetary tightening (easing) during booms (slowdowns).

I adopt an empirical approach. In particular, I study the dynamic effects across economic states of a structural monetary policy shock on four downside risk measures (i.e., Uncertainty, Downside Uncertainty, Macro Skewness, Growth-at-Risk), derived linearly combining relevant quantiles of the conditional expected distribution of output growth. As in Forni et al. (2023), the dynamic responses of quantiles of the predicted density to structural shocks are obtained combining coefficients associated to a VAR and quantile regressions. However, I extend the original framework by substituting constant coefficients with smooth-transition parameters in order to account for state dependence. Specifically, I recover state-dependent quantile impulse response functions (QIRFs) combining mean IRFs, recovered from the estimation of a smooth-transition VAR, and obtaining the coefficients of the combination estimating a smooth-transition quantile regression. Then, the downside risk response to the shock is computed linearly combining state-dependent QIRFs, according to the definition of each of the four indicators. Effectively, instead of computing conditionally (on the state) linear QIRFs, I rely on generalized QIRFs conditioning only on the state in place when the shock hits and allow endogenous state transition throughout the response forecast horizon. The approach to compute state dependent QIRFs proposed in this paper is quite flexible, as it consents to obtain responses across a continuum of states and quantiles without the need of any distributional assumption that would constrain quantile dynamics. Moreover, it is computationally efficient, can be estimated in a single step and it delivers easily interpretable results. I identify monetary policy shocks using the instrument of Miranda-Agrippino and Ricco (2021). The data used covers the US for the period 1973m1:2019m12.

I find that expansionary monetary policy is effective in reducing downside risks to the economy during recessions. On the other hand, monetary contractions implemented during booms significantly increase risk. Crucially, however, monetary interventions cause risk

responses about four times bigger in size, if the shocks occur during economic slowdowns instead of booms (given the same magnitude of the shock).[1] In addition, I find that responses of downside risk in recession almost overlap with those obtained using the constant parameter model of Forni et al. (2023). On the contrary, linear IRFs are about four times higher than those computed conditioning on an expansionary state of the economy. This evidence has important policy implications. Specifically, policy interventions calibrated on linear (i.e., average) estimates would lead to an over-cautious behavior of monetary policymakers (i.e., monetary tightening during booms would be too conservative). Interestingly, the result holds also when looking at unexpected monetary contractions occurring during booms associated to high private credit to GDP levels. Regarding the transmission mechanisms, in line with the existing literature, I find that movements in the left tail are the main drivers of variations in the shape of the expected density of output growth; in addition, I show that the lowest quantiles of the density respond more pronouncedly to monetary policy shocks occurring during slowdowns. Consequently, the state asymmetries in the responses of downside risk measures (linear combinations of the 5^{th}, 50^{th}, 95^{th} quantiles of the expected density) can be explained by the discrepancy in the GaR (5^{th} quantile) responses in expansions and recessions. Moreover, evidence proposed in this paper suggests that financial conditions are a key driver of the asymmetric transmission of monetary policy shocks to downside risk across economic states. I also find that monetary policy is able to explain a relevant share of variations in downside risk. In this regard, variance decomposition shows that unexpected monetary interventions in recessions account for up to 20% of variations in the shape of the predicted density of output growth on impact and 25% at longer horizons. On the other hand, variance explained by monetary policy shocks occurring during booms is rather similar on impact, but only around 10% at longer horizons.

Related literature. This paper relates to three strands of the literature.

First, my work closely speaks to a very recent methodological literature analyzing the causal link between structural shocks and (quantiles of) predicted distributions. In particular, Forni et al. (2023) combine structural VARs and quantile regressions, finding that a contractionary monetary policy shock affects the predicted density of output growth by increasing its dispersion and by moving mass to the left tail. Similarly, Loria et al. (2022) couple quantile regressions and local projections, reaching the same conclusions. Along similar lines, Caldara et al. (2021) recover the forecast density of output growth from a Markov-switching VAR, confirming and rationalizing previous results. Instead, Chavleishvili et al. (2021) propose a quantile VAR and study the effects of macro-prudential policy on downside risk. The methodological contribution of my work is to extend the model of Forni et al. (2023) to account for state-dependence, combining a smooth-transition VAR and smooth-transition quantile regressions.

Second, there is an empirical literature studying the asymmetric impact of monetary policy shocks in expansions and recessions. Despite robust evidence in favor of the existence of a state dependence, finding in terms of the direction of the asymmetry a still very far from being univocal. In particular, Bruns and Piffer (2023) use an ST-VAR, directly estimating transition parameters and identifying shocks using the instrument of Gertler

[1] The asymmetry holds when looking at mean responses. These results are in line with the financial accelerator literature.

and Karadi (2015), to find that monetary policy is more effective in recession. The same conclusion is reached by Peersman and Smets (2001), Garcia and Schaller (2002), Lo and Piger (2005) using Markov-switching multivariate models. The results of Debortoli et al. (2023) go along the same lines. On the other hand, Tenreyro and Thwaites (2016) exploit smooth transition local projections and a narrative identification à la Romer and Romer (2004), obtaining diametrically opposite results. The same conclusion is defended in Jordà et al. (2020), modelling panel instrumental variable local projections and exploiting a quasi-natural experiment, and in Alpanda et al. (2021), exploiting panel threshold local projections and sign restrictions.[2] I contribute to this literature by bringing evidence that sustains the claim of higher effectiveness of monetary policy during economic slowdowns. In addition, I show that this conclusion holds when looking to moments beyond the mean.

Finally, this work speaks to a literature focusing on the estimation of the conditional forecast density of output growth. The seminal work is Adrian et al. (2019), who obtain the conditional distribution semi-parametrically estimating quantile regressions and fitting predicted quantiles into skewed-t distributions. More recently, Plagborg-Møller et al. (2020) test various predictive models, concluding that forecasts of moments beyond the first should be looked at cautiously because they tend to be imprecisely estimated. On the other hand, Cho and Rho (2023) confirm the robustness of Adrian et al. (2019) results. Another recent work is Wolf (2021), who proposed a fully parametric skewed stochastic volatility model to estimate GaR, finding results similar to those of the seminal paper. Other relevant recent works are Clark et al. (2024) and Delle Monache et al. (2023). I contribute to this literature by extending the model of Adrian et al. (2019) allowing the predictive power of regressors in quantile regressions to vary with the state of the economy.[3]

The rest of the paper is structured as follows. Section 2 describes the econometric approach, Section 3 presents the main results and Section 4 discusses some robustness exercises. Finally, Section 5 provides few concluding remarks.

2 Econometric approach

This section describes the empirical approach proposed in this paper. First, I present the definition of downside risk adopted in this work. Second, I describe the econometric method used to recover the response of downside risk to monetary policy shocks, across economic states. Third, I linger on the estimation procedure and on the data used.

2.1 Downside risk

I consider four different indicators to proxy macroeconomic downside risk, all defined as linear combinations of relevant quantiles of the conditional expected density of output growth, x_t^τ. More in detail, downside risk measures are defined as follows. "Uncertainty" is computed approximating the dispersion of the expected density of output growth (i.e., difference

[2] The recent contribution of Gonçalves et al. (2023) calls into question results obtained using state dependent local projections.

[3] My contribution to this literature is functional to the extension of the model of Forni et al. (2023) and improving forecasting accuracy is beyond the scope of this paper.

between the 95^{th} and the 5^{th} quantiles)

$$\mathcal{U}_t = x_t^{95} - x_t^5 \tag{1}$$

Next, following the intuition of Forni et al. (2024), I decompose Uncertainty and consider only its downside component, named "Downside Uncertainty", which is defined as the dispersion of the left portion of the density

$$\mathcal{D}_t = x_t^{50} - x_t^5 \tag{2}$$

Relating to a recent literature on skewed business cycles (Iseringhausen et al. (2023)), I proxy the third moment of the conditional forecast density of output growth looking at the difference between its left and right portions (Kelley (1947)), and define "Macro Skewness" as

$$\mathcal{S}_t = (x_t^{50} - x_t^5) - (x_t^{95} - x_t^{50}) \tag{3}$$

Finally, referring to the seminal paper of Adrian et al. (2019), I define Growth-at-Risk (GaR) as the negative of the 5^{th} quantile of the density

$$\mathcal{GAR}_t = -x_t^5 \tag{4}$$

Note that all measures are defined such that any increment in these indicators is to be interpreted as an increase in (downside) risk. There are few advantages related to the adopted definitions. First, they consent to summarize the shape of the expected density of output growth in few meaningful objects, without the need of distributional assumptions on x_t. Second, they allow to explain variations in risk measures by looking directly to the dynamics of their defining components (i.e., quantiles). Third, as different measures of downside risk explored in the literature are usually found to be highly correlated, the proposed definition consents to uncover an additional layer and investigate whether co-movements are driven by the same factors (i.e., quantiles). The main limitation is that quantiles are not observed. This means that recovering them and studying their state-dependent dynamics in response to monetary policy shocks requires a dedicated econometric framework, which is described in the next section.

2.2 State-dependent (linear combination of) quantile IRFs

In this section, I describe how I recover the state-dependent dynamic response of quantiles of a distribution of interest to structural shocks. Next, given the definition of downside risk measures proposed above, I show how to extend the econometric framework to recover state-dependent IRFs of linear combinations of quantiles.

State-dependent quantile IRFs. I compute state-dependent quantile IRFs by extending the model proposed in Forni et al. (2023) to account for state asymmetries. Specifically, as in the reference paper I combine quantile regressions and structural VAR, but I decline both in a state-dependent fashion featuring smooth-transition parameters. Details are outlined below.

First, expanding the quantile forecasting model of Adrian et al. (2019) I assume that,

conditional on the state of the economy, quantiles of a distribution of interest can be obtained as a linear combination of predictors. Formally,

$$\begin{aligned} x_t^\tau &= \beta'_{\tau,s}(L) W y_t \\ \beta'_{\tau,s}(L) &= f(z_{t-1})\beta'_{\tau,R}(L) + (1 - f(z_{t-1}))\beta'_{\tau,E}(L) \\ f(z_t) &= \frac{e^{-\phi z_t}}{1 + e^{-\phi z_t}} \end{aligned} \tag{5}$$

where x_t^τ is the quantile τ of the distribution of interest and y_t is a vector of predictors. The selection matrix W is composed of zeros and ones and it allows impose a null coefficient on selected predictors.[4] The state-dependence of the vector of polynomials in the lag operator, $\beta'_{\tau,s}(L)$, is obtained as a convex combination of coefficients associated to "limit" states, $\beta'_{\tau,R}(L)$ and $\beta'_{\tau,E}(L)$, which for convenience I define as recession and expansion. The parameters of the convex combination are defined by a logistic transition function $f(z_t)$ which takes as input an observed state indicator z_t.[5] The parameter ϕ governs the smoothness of the transition from one "limit" state to the other. Summarizing, $\{x_t, y_t, z_t\}$ are observed data, whereas $\{\beta'_{\tau,R}(L), \beta'_{\tau,E}(L), \phi\}$ are the parameters of the model.[6]

Second, I assume that the vector of predictors y_t in Equation 5 has an invertible smooth-transition vector moving average (ST-VMA) representation, such that this can be recovered estimating a smooth-transition VAR (ST-VAR) from observed data. Formally, I define the process governing y_t as

$$\begin{aligned} y_t &= B_s(L) y_t + \xi_t \\ B_s(L) &= f(z_{t-1})B_R(L) + (1 - f(z_{t-1}))B_E(L) \end{aligned} \tag{6}$$

where y_t (defined as in Equation 5) is a vector of endogenous variables and ξ_t is the error term. Mirroring Equation 5 in a multivariate setting, the state-dependence of the matrix of coefficients in the lag operator $B_s(L)$ is parameterized as a convex combination of coefficients associated "limit" states, $B_R(L)$ and $B_E(L)$. The definition and interpretation of the transition function $f(z_t)$ is exactly the same as in Equation 5. Now, given invertibility, the ST-VAR can be expressed in its structural ST-VMA representation, as follows

$$y_t = C_s(L) H \zeta_t \tag{7}$$

where $C_s(L) = (I - B_s(L))^{-1}$ is a matrix of reduced-form state-dependent IRFs, $\zeta_t = H^{-1}\xi_t$ is a vector of structural shocks and H is the impact matrix used to recover structural parameters.

Third, combining Equations 5 and 7 one can obtain an expression that defines the

[4] The matrix W is not essential and can be set to be an identity; it is used to allow for a parsimonious specification.

[5] I use a lagged value of $f(z_t)$ to compute the weights of the linear combination in order to avoid contemporaneous feedback on whether the economy is in a recession (i.e., shocks are allowed to affect the state of the economy only one period after they hit).

[6] Finally, note that since the elements of the vector of coefficients are polynomials in the lag operator, the model in Equation 5 can be thought as a conditional quantile forecasting model, where the influence of predictors is allowed to change with the state of the economy.

quantile x_t^τ as a linear combination - different in each state of the economy - of structural shocks. Formally,

$$x_t^\tau = [\beta'_{\tau,s}(L)WC_s(L)H]\zeta_t \tag{8}$$

where the element in squared brackets denotes state-dependent quantile IRFs. The intuition behind Equation 8 is that quantiles of a variable of interest can be obtained combining a set of predictors, which in turn respond dynamically to structural shocks, allowing to trace a direct link between shocks and quantiles. In other words, the mapping from structural shocks to quantiles, $\beta'_{\tau,s}(L)WC_s(L)H$, is nothing else than a state-dependent linear combination, $\beta'_{\tau,s}(L)W$, of state-dependent structural mean IRFs, $C_s(L)H$.

State-dependent (linear combination of) quantile IRFs. The econometric framework used to obtain state-dependent quantile IRFs described above can be relatively easily adapted to obtain state-dependent IRFs for linear combinations of quantiles, hence downside risk measures. To see how, consider a generic linear combination of quantiles of x_t

$$\begin{aligned} q_t &= ax_t^{\tau_a} + bx_t^{\tau_b} - cx_t^{\tau_c} \\ &= a\beta'_{\tau_a,s}(L)Wy_t + b\beta'_{\tau_b,s}(L)Wy_t - c\beta'_{\tau_c,s}(L)Wy_t \\ &= \underbrace{[a\beta'_{\tau_a,s}(L) + b\beta'_{\tau_b,s}(L) - c\beta'_{\tau_c,s}(L)]}_{\beta'_{\tau_{abc},s}(L)}WC_s(L)H\zeta_t \end{aligned} \tag{9}$$

where the first equality defines the generic linear combination of quantiles, the second uses Equation 5 to substitute each x_t^τ and the third exploits Equation 7 to substitute y_t. Equation 9 describes a state-dependent mapping from structural shocks to combination of quantiles, which is nothing else than an impulse response function. Now, note that $WC_s(L)H$ is independent of quantiles, hence it suffices to modify *ad hoc* the generic $\beta'_{\tau,s}(L)$ in Equation 8 with $\beta'_{\tau_{abc},s}(L)$ to obtain the IRFs of interest. Then, given the above and the definition of downside risk measures presented in the previous section, it is straightforward to see that simply substituting the following

$$\begin{aligned} \beta'_{\mathcal{U},s}(L) &= \beta'_{0.95,s}(L) - \beta'_{0.05,s}(L) \\ \beta'_{\mathcal{D},s}(L) &= \beta'_{0.50,s}(L) - \beta'_{0.05,s}(L) \\ \beta'_{\mathcal{S},s}(L) &= (\beta'_{0.50,s}(L) - \beta'_{0.05,s}(L)) - (\beta'_{0.95,s}(L) - \beta'_{0.50,s}(L)) \\ \beta'_{\mathcal{GAR},s}(L) &= -\beta'_{0.05,s}(L) \end{aligned} \tag{10}$$

in place of the generic $\beta'_{\tau,s}(L)$ in Equation 8 is enough to obtain state-dependent IRFs for Uncertainty, Downside Uncertainty, Macro Skewness and GaR, respectively.

2.3 Estimation and data

The parameters needed to recover IRFs are $\Psi = \{\beta'_{\tau,R}(L), \beta'_{\tau,E}(L), B_R(L), B_E(L), \phi, W, H\}$, whereas observed data are $D_t = \{x_t, y_t, z_t\}$.

Reduced-form parameters. The parameters to be estimated consist in all the elements belonging to Ψ, except from W and H, which are obtained pre-estimation and post-estimation, respectively. Estimation in performed as follows. First, notice that given the

smooth-transition parametrization of state dependence, conditional on the state s, quantile IRFs can be obtained via a linear combination, $\beta'_{\tau,s}(L)$, of VMA coefficients, $C_s(L)$. In the linear baseline model (i.e., assuming constant parameters), these two objects can be estimated separately, as they are independent. Specifically, $\beta'_{\tau}(L)$ can be estimated via quantile regression, whereas $C(L)$ is obtained inverting an estimated VAR (Forni et al. (2023)). Now, when extending the model to incorporate state-dependence, parameters $\beta'_{\tau,s}(L)$ and $C_s(L)$ are correlated because they are both a function of the smoothness parameter ϕ, hence they should be estimated jointly. However, specifying a joint likelihood is cumbersome and would require distributional assumptions that would constrain quantile dynamics, significantly reduce the scope of the analysis. Instead, I opt for a more agnostic estimation procedure. Specifically, I exploit the fact that, conditional on ϕ, Equations 5-6 become linear in coefficients, such that $\{\beta'_{\tau,R}(L), \beta'_{\tau,E}(L)\}$ and $\{B_R(L), B_E(L)\}$ are independent, and hence can be estimated separately using the standard constant-parameters quantile regression estimator (Koenker and Bassett Jr (1978)) and OLS, respectively. Formally, quantile regression coefficients for quantile τ, conditional on ϕ, are obtained as follows

$$\tilde{\beta}'_{\tau,\phi}(L) = \underset{\tilde{\beta}'_{\tau,\phi}(L)}{\arg\min}\, L_{qr} = \underset{\tilde{\beta}'_{\tau,\phi}(L)}{\arg\min} \sum_{t=1}^{T} (\mathbb{1}_{(\eta^{\tau}_{t,\phi} \geq 0)} |\eta^{\tau}_{t,\phi}| \tau + \mathbb{1}_{(\eta^{\tau}_{t,\phi} < 0)} |\eta^{\tau}_{t,\phi}| (1-\tau)) \tag{11}$$

where $\eta^{\tau}_{t,\phi} = x_t - \tilde{\beta}'_{\tau,\phi} \tilde{y}_{t,\phi}$ and $\tilde{\beta}'_{\tau,\phi} = \begin{bmatrix} \beta'_{R,\tau,\phi}(L) & \beta'_{E,\tau,\phi}(L) \end{bmatrix}$ and $\tilde{y}_{t,\phi} = \begin{bmatrix} \frac{e^{-\phi z_t}}{1+e^{-\phi z_t}} y_t \\ (1 - \frac{e^{-\phi z_t}}{1+e^{-\phi z_t}}) y_t \end{bmatrix}$ and $\mathbb{1}_{()}$ is an indicator function that takes value 1 if the condition in parenthesis is satisfied, 0 otherwise. Similarly, conditional on ϕ, VAR coefficients can be obtained minimizing the standard OLS loss function

$$\tilde{B}_{\phi}(L) = \underset{\tilde{B}_{\phi}(L)}{\arg\min}\, L_{var} = \underset{\tilde{B}_{\phi}(L)}{\arg\min} \sum_{t=1}^{T} (\xi'_{t,\phi} \xi_{t,\phi}) \tag{12}$$

where $\xi_{t,\phi} = y_t - \tilde{B}_{\phi}(L) \tilde{y}_{t,\phi}$ and $\tilde{B}_{\phi}(L) = \begin{bmatrix} B_{R,\phi}(L) & B_{E,\phi}(L) \end{bmatrix}$ and $\tilde{y}_t$ is defined as above. Now, exploiting the model conditional (on the state) linearity, I obtain an estimate for ϕ via grid-search (Lerman (1980)).[7] More in detail, I define a joint conditional (on ϕ) QR-VAR loss function as the sum of the conditional "standardized" QR and VAR loss functions described in Equations 11-12. Then, the estimate for ϕ is obtained as the value - within a finite and discrete uni-dimensional pre-specified gird Φ - that minimizes the conditional QR-VAR loss function

$$\phi^* = \underset{\phi \in \Phi}{\arg\min} (\tilde{L}_{qr} + \tilde{L}_{var}) \tag{13}$$

Note that the QR and VAR conditional loss functions are intrinsically different, hence hardly comparable. In order to overcome this limitation, I exploit the discrete nature of the grid-search approach and consider their standardized version, $\tilde{L}_{qr}$ and $\tilde{L}_{var}$. Operationally, I obtain two vectors $\bar{L}_{qr}$ and $\bar{L}_{var}$, where each entry corresponds to the value associated to the conditional loss functions evaluated at a certain ϕ, and standardize them. Doing so, I obtain two vectors that give information on how different values of ϕ perform in terms of

[7] See Bruce (1997) for an application to threshold VARs.

normalized deviations from the neutral performance, *de facto* "controlling" for the different nature of QR and VAR conditional loss functions. Finally, once ϕ^* is obtained, coefficients $\tilde{\beta}'_{\tau,\phi^*}(L)$ and $\tilde{B}_{\phi^*}(L)$ are recovered using expressions 11-12.

Selection matrix. The matrix W is chosen pre-estimation of reduced-form parameters described above. The rational for the inclusion of W in the model is twofold. First, it allows to perform quantile regression estimation on a subset of the VAR regressors, allowing for flexibility. Second, by imposing ex-ante a zero coefficient on certain quantile regression predictors, the selection matrix allows for parsimony and eases interpretation of results. Now, the criterion to pin-down the elements of W is the following. Non-zero coefficients in state-dependent quantile regression are allowed only for predictors whose associated coefficients in linear quantile regressions are statistically significant at least at the 15% level in each of the three quantile regressions used to compute downside risk measures (i.e., for $\tau = 0.05, 0.5, 0.95$). The intuition is that including regressors whose predictive power direction is very much uncertain is very likely to result in bad forecasts.

Identification. The matrix H is pinned-down post estimation, combining reduced-form VAR residuals, their covariance matrix and an external instrument. Specifically, I identify structural shocks following the procedure proposed in Gertler and Karadi (2015).[8]

Generalized IRFs. The state-dependent quantile IRFs defined in Equation 8, conditional on the state, are a linear combination of structural shocks. This implies an implicit assumption on the fact that the economic state in place when the shock hits remains the same throughout the forecast horizon. In order to overcome such imposed constraints on post-shock quantile dynamics, I opt to rely on generalized IRFs (GIRFs) à la Koop et al. (1996), which allow to condition only on the state in place when the shock hits, but consent shifts across states to evolve endogenously along the forecast horizon. Formally, GIRF for quantile x^τ is defined as

$$GIRF_{x^\tau}(h, \delta, \lambda) = \mathbb{E}[x^\tau_{t+h}|\delta, \lambda_t] - \mathbb{E}[x^\tau_{t+h}|\delta = 0, \lambda_t] \tag{14}$$

where h is the response forecast horizon, δ is the size of the shock and λ_t represents the economic condition when the shock hits (or, initial conditions). Differently from conditionally linear IRFs, GIRFs do not have a fully parametric expression, and hence are obtained via simulations. Specifically, $\mathbb{E}[x^\tau_{t+h}|(\delta), \lambda_t]$ is obtained via an iterated forecast for h periods, which starts using predictors realized at time t (i.e., λ_t). Then, the forecast distribution for a specific λ_t (i.e., economic state) is recovered repeating the forecast F times, each time drawing a vector of VAR residuals for each forecast iteration.[9] Note that parameters Ψ are treated as fixed in the forecast exercise, hence do not directly account for estimation uncertainty. The simulation algorithm is described more in detail in Appendix C.3.[10]

[8] Note that the impact matrix is not state-dependent. See Appendix C.2 for more details.

[9] I do not assume any distribution for ξ_t, therefore I opt for a form of bootstrap procedure.

[10] Accordingly, I calculate generalized forecast error variance decompositions (GFEVD), as proposed in Lanne and Nyberg (2016) and Caggiano et al. (2017). See Appendix C.4 for the definition and computation algorithm.

Data. I include in y_t 4 blocks of variables: policy (1-year nominal interest rate)[11], real (log industrial production and unemployment rate), financial (National Financial Condition Index, log SP500 stock prices index, private credit to GDP), prices (log consumer price index).[12] Next, I define the state variable z_t to be a standardized 2-months backward-looking moving-average of the growth rate of industrial production.[13] Finally, the variable whose quantile dynamics are of interest of this paper, x_t, is chosen to be a 3-months ahead industrial production growth. The data cover the US for the period 1970m1:2019m12. As for the instrument used to identify structural shocks, I adopt the one proposed in Miranda-Agrippino and Ricco (2021), extended in Degasperi and Ricco (2021) to cover the period 1991m1:2017m12.

3 Results

This section presents and comments the main findings of the paper. First, I show the baseline results. Then, I explore potential transmission mechanisms that may rationalize the benchmark results. Finally, I present the output of an exercise in which I look at the response of downside risk to a contractionary monetary policy shock hitting during an economic expansion associated to a high private credit to GDP level.

3.1 Baseline results

Figure 1 plots the downside risk measures defined in Section 2.1, estimated using the quantile forecasting model presented in Equation 5.

Figure 1: Risk measures - Estimates

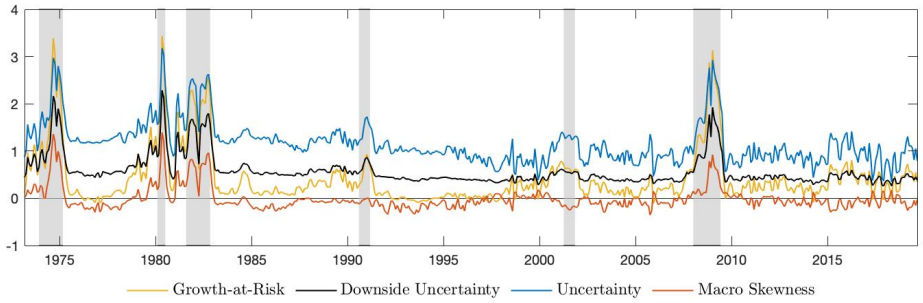

This figure plots the estimated downside risk measures; vertical shaded bands indicate NBER recessions.

All the estimated indicators appear relatively flat during normal times, whereas they spike during recessions. Series are particularly highly correlated, suggesting that there may

[11] I use the 1-year nominal interest rate as the policy rate to account for the zero lower bound period, following the approach of Gertler and Karadi (2015) and Miranda-Agrippino and Ricco (2021).

[12] Including financial conditions indicators relaxes concerns regarding invertibility, a key condition for the identification strategy to be valid (Forni et al. (2022)).

[13] I choose a window of two months for the moving average to maintain a similar information set as for the VAR lags. The window is the same as Bruns and Piffer (2023).

exist a common factor driving the co-movements.[14] Growth-at-Risk (i.e., left tail of the density) is the most volatile among the risk measures and it is the main driver of variations in the other series.[15] Overall, evidence presented in Figure 1 is in line with the existing literature. Specifically, during economic downturns there is a drop in the first moment of the predicted density, coupled by a a spike in uncertainty (i.e., second moment) mostly driven by its downside component. In turn, this implies that the density becomes more left-skewed (i.e., increase in the third moment). Variations in the shape of the expected density are majorly driven by fluctuations in its left tail.

Figure 2: Risk measures - Impulse Response Functions

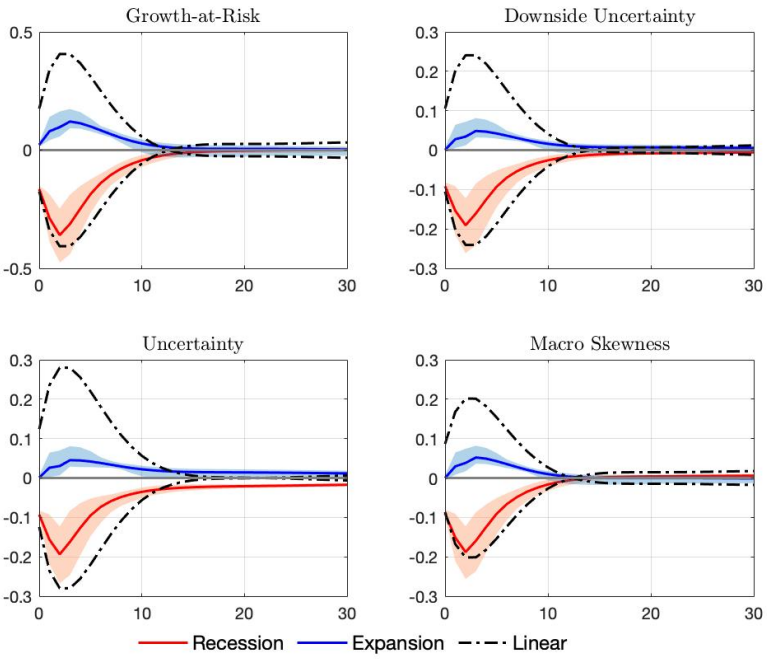

This figure plots the IRFs to a monetary policy shock of risk measures. Red (blue) lines denote average responses in recession (expansion). Confidence bands are reported at the 90% level. Dash-dotted black lines indicate IRFs obtained using the benchmark linear model of Forni et al. (2023).

Now, if Figure 1 presents an overview of the downside risk outlook over time, Figure 2 provides insights on the ability of monetary policy to drive its dynamics.[16] In particular, it shows the response of downside risk to an expansionary (contractionary) monetary policy in recession (expansion), calibrated to cause a drop (increase) of 50 basis points on impact in the policy rate. Blue (red) lines indicate the responses of risk measures, conditional on the

[14] See Table 3 in Appendix B.

[15] The average variation between two consecutive periods in the 5^{th} quantile is 1.5 and 2.5 times the average variation in the median and in the 95^{th} quantile, respectively. As downside risk measures are obtained as combinations of such quantiles, it follows that tail tail risk is the main driver of variations in the other risk measures. See Figure 7 in Appendix A for graphical evidence.

[16] See Appendix C.1 for the response of the full density, across states.

shock hitting during booms (recessions).[17] Dash-dotted black lines indicate IRFs obtained using the benchmark linear model of Forni et al. (2023). Evidence presented in Figure 2 shows that an expansionary monetary policy shock hitting during recessions is effective in reducing downside risk. On the other hand, a monetary contraction occurring during booms increases risk. Nonetheless, given a same size shock, the magnitude of the increase in risk following a monetary contraction in expansion is about four times smaller than the reduction in risk in the aftermaths of an loosening shock during slowdowns. In addition, notice that the responses of downside risk in recession almost overlap with those obtained using the constant parameter model of Forni et al. (2023).[18,19] This evidence has important policy implications. Specifically, policy interventions calibrated on linear (i.e., average) estimates would lead to an over-cautious behavior of monetary policy-makers. Specifically, basing policy on average parameters would lead to over-conservative tightenings during booms. However, notice that mean responses reported in Figure 8, Appendix A, show that also real variables and prices respond asymmetrically across states.[20] This means that, for instance, to achieve a reduction in inflation during a boom with a tightening intervention of the same magnitude of the increase that an easing policy during a recession would have generated, the size of the shock should be bigger; this in turn implies that the increase in downside risk would be higher. In practice, central banks face an inflation-risk trade-off.

Finally, if Figure 2 shows that monetary policy is indeed able to drive some of the dynamics of downside risk, it is still to be defined how relevant is monetary policy in explaining overall dynamics. A potential answer can be gauged looking to the forecast error variance decomposition. The GFEVD presented in Table 1 suggests that monetary policy accounts for a relevant share of total variations in the shape of the predicted density of output growth, hence in downside risk. Overall, the variance explained by monetary policy shocks is systematically higher during economic slowdowns, compared to expansions. In absolute terms, monetary interventions explain about 20% of the variations on impact in downside risk indicators during recessionary times, slightly less during booms. At longer horizons, the variance explained during economic downturns increases to 25%, whereas it decreases to about 10% during expansions. Finally, note that monetary policy is found to explain relatively low shares of variation in real variables, however it plays an important role in shaping expectations (i.e., moments of the forecast distribution of output growth).[21]

[17] I cluster in the recession (expansion) set all GIRFs obtained from an initial condition in which the value of the associated transition function is in its top (bottom) percentiles. This means that I compare the responses of risk measures to monetary policy shocks in deep recessions and sustained booms. Results qualitatively hold when I consider milder recessions and booms (see Section 4).

[18] This is in line with the fact that most of variations in the risk measures occur during recession, as highlighted in Figure 1.

[19] Note that linear IRFs are not imposed to lie in between GIRFs in expansion and recession. The reason is twofold. First, GIRFs are obtained via simulation and the continuous lines plotted in Figure 2 are averages of selected simulations. Second, when considering GIRFs, the mapping form mean response to quantile responses is non-linear.

[20] These results can be rationalized by models featuring a "financial accelerator" mechanism. Overall, results for mean responses are in line with those of Bruns and Piffer (2023), who use a similar methodology to account for state-dependence in the effects of monetary policy.

[21] The GFEVD for the ST-VAR variables is reported in Table 4, Appendix B

Table 1: Generalized forecast error variance decomposition

	$h = 0$		$h = 12$		$h = 24$	
	Recession	Expansion	Recession	Expansion	Recession	Expansion
Growth-at-Risk	18.52	23.58	25.59	9.47	25.40	8.94
Uncertainty	20.63	9.89	26.22	10.04	25.96	9.30
Downside Uncertainty	20.69	15.17	26.21	10.69	25.57	9.65
Macro Skewness	20.57	18.67	26.15	8.54	26.11	7.90

This table shows the the variance of variables of interest explained by the monetary policy shock at different forecast horizons, across states.

3.2 Transmission mechanisms

The baseline results presented in the previous section show that monetary policy is able to drive downside risk and that this ability is higher during economic downturns. However, evidence so far is still muted with respect to the potential drivers of such causal relation. This section aims to fill this gap by shedding some additional light on possible transmission mechanisms.

The risk measures responses to a monetary shock presented in Figure 2 appear very highly correlated, suggesting that there may exist a common driver. Given the relevance of GaR in explaining variations in the other risk indicators over time highlighted in Figure 1, tail risk arises as the natural candidate. In order to explore whether this is the case, I "unpack" risk measures and look directly to the responses of their components. In particular, I compare the response of quantiles whose linear combination defines the risk measures of interest. Figure 3 plots the responses of a set of representative quantiles of the forecast density to the same monetary policy shock (note that I flip the sign of the responses in expansion, to ease the size comparison).[22] The left (right) panel shows quantile responses, conditional on the shock hitting in a recession (expansion). As above, the size of the structural shock is calibrated such that the policy rate declines (increases) by 50 basis points on impact on average. Results show that the 5^{th} quantile of the forecast distribution of output growth is more responsive to the shock than the median and the 95^{th} quantile, in both states. This means that changes in the shape of the density can be largely explained by the more pronounced shift of the left tail, compared to that of the median and the right tail. In particular, the gap between the shift of the left and right tails explains the movement in Uncertainty. Instead, the variations in Macro skewness is due to the fact that the responses of the right tail and the median are very similar, implying that the shape of the right side of the density experiences only minor variations; the opposite applies to the left side, as the left tail increases more than twice compared to the median. Now, notice that the difference between the response of the left tail and those of the median and the right tail is much more pronounced during economic downturns. This means that variations in the shape of the forecast density - hence in the risk measures - are deeper during slumps and that the

[22] See Figure 9 for the response of more quantiles to the shock, across states.

source of this asymmetry is the variation in the left tail, i.e., Growth-at-Risk.

Figure 3: Quantiles - Impulse Response Functions

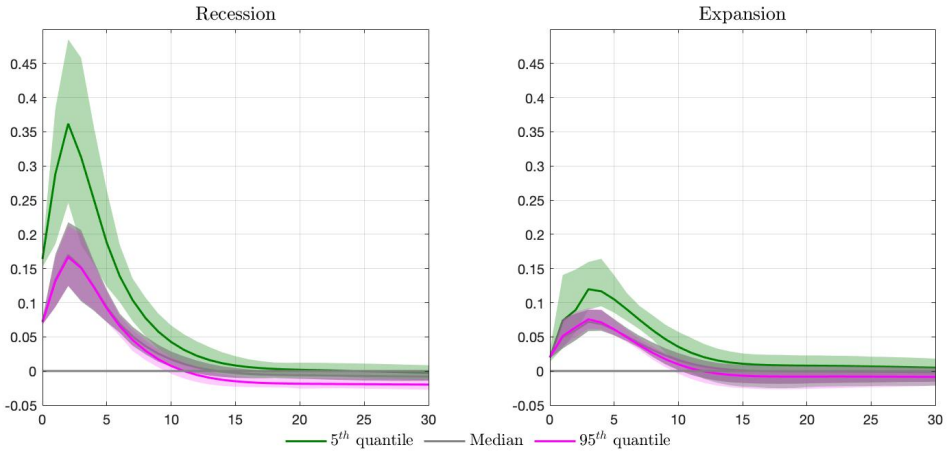

This figure plots representative quantile IRFs to a monetary policy shock, conditional on the monetary intervention occurring in recession or expansion.

In turn, the state-dependent response of tail risk to the monetary shock can be explained by the the asymmetric response of NFCI across states (see Figure 8), as Tables 5-6 suggest that NFCI is by far the most important predictor of tail risk and that its relevance is higher in recessions. Summarizing, evidence proposed in this paper points to the following transmission mechanism: 1) monetary policy has an asymmetric effect on NFCI; 2) NFCI is a very strong predictor of GaR, implying its state-dependent response; 3) tail risk response is a major driver of uncertainty and skewness responses, causing such responses to be asymmetric across states.[23]

Table 2: Quantile regression - Selected regressors

	$\tau = 0.05$		$\tau = 0.5$		$\tau = 0.95$	
	Recession	Expansion	Recession	Expansion	Recession	Expansion
NFCI	-0.82	-0.12	-0.35	-0.13	-0.35	-0.09
SP500	0.00	0.00	0.00	0.00	0.00	0.00
(lag) Policy rate	0.04	0.02	-0.01	0.00	0.00	0.00

This table reports estimated quantile regression coefficients, after the selection of relevant regressors.

[23] See Adrian et al. (2020) for a theoretical model embedding tail risk.

3.3 Does leverage matter?

In this section, I focus on whether the occurrence of a monetary policy shocks during a boom has different impacts based on whether the expansions is associated with a high private credit to GDP level. Figure 4 suggests that risk in highly-leveraged states of the economy responds indistinguishably from unconditional booms.

Figure 4: IRFs - Booms and high credit/GDP

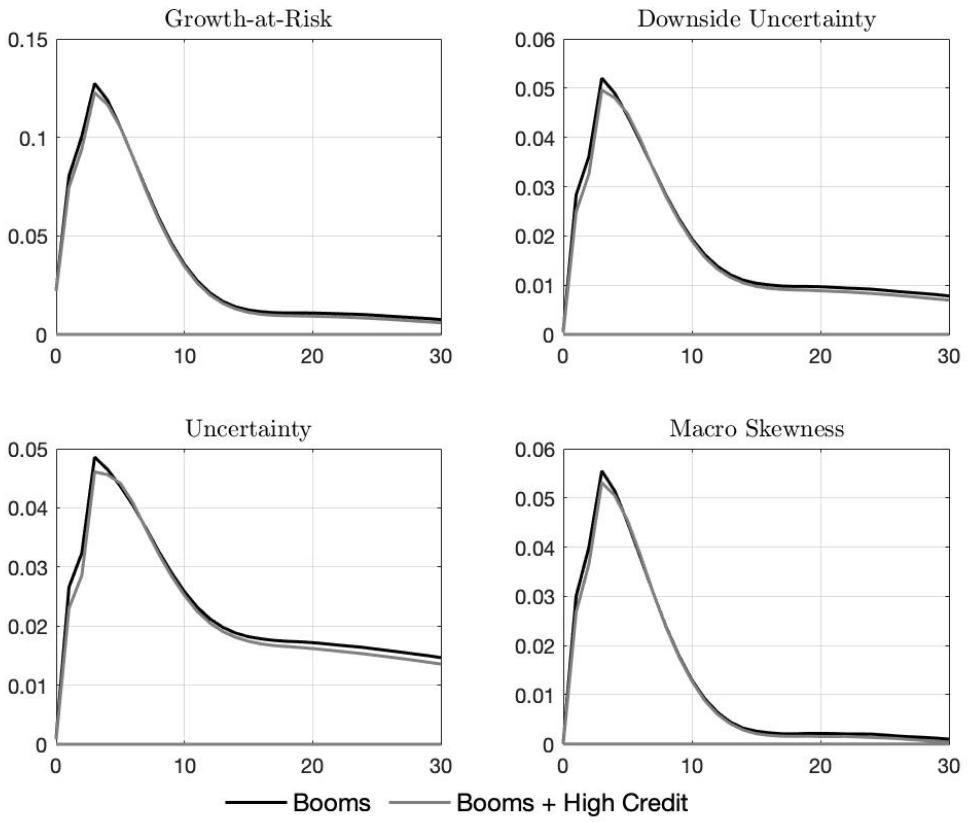

This figure plots the response of downside risk indicators to a contractionary monetary policy shock. Black lines are baseline responses during booms; grey lines indicate responses during booms associated to high private credit to GDP levels.

4 Robustness

In this section, I check the robustness of the empirical results presented in Section 3 against a battery of tests. I gather tests based on which component of the quantile IRF (i.e., $\beta'_{\tau,s}(L)WC_s(L)H$) they affect.

First, I perform three modifications concerning $\beta'_{\tau,s}(L)$. First, I change the "tail" quantiles used to build proxies for the moments of the forecast density (i.e., I use $\tau = \{0.1, 0.9\}$, instead of $\tau = \{0.05, 0.95\}$). Second, I change the horizon of the forecast density from three

to six months. Third, I impose no state-dependence in the combination of mean IRFs to obtain quantile IRFs; practically, I impose $\beta'_{\tau,s}(L) = \beta'_{\tau,R}(L) = \beta'_{\tau,E}(L)$ and obtain coefficients estimating a linear quantile regression. The output of this first set of robustness exercises in reported in Figure 10. On top of reassuring on the robustness of the empirical exercise, stability of results vis-à-vis the changes described above provides also relevant insights. In particular, results obtained using a linear quantile forecasting model are quantitatively very similar to the ones obtained adopting a smooth-transition framework. This implies that most of the state asymmetries in the dynamics of risk responses described in Section 3 can be explained by the asymmetric responses of mean variables during booms and recessions, rather than their non-linear combination. On the contrary, the asymmetry across states of GaR risk measures responses on impact is entirely driven by the non-linearity coming from ST-QR, by construction.

Second, I change the composition of the W matrix, in two ways. First, I select as predictors to be included in Equation 5 all variables whose associated coefficient in a linear quantile regression is statistically significant at the 5% level for at least one of the three relevant quantiles used to compute proxies for the moments of the density (i.e., $\tau = 0.05, 0.5, 0.95$). Second, I set W equal to the identity matrix, essentially including in Equation 5 all variables part of the vector y_t and their lags. Results are reported in Figure 11. Varying the set of predictors does not qualitatively change the results at short and long IRF forecast horizons. However, variations cause the response of risk measures to the shock on impact to be different form the baseline results. That said, one should cautiously interpret the output of this robustness exercise. In particular, using predictors whose coefficients are imprecisely estimated can lead to misleading results. This is precisely the reason why I included the selection matrix W in the baseline model in Equation 5.

Third, I relax the bounds I use to define recessions and expansions, which ultimately determine the set of initial conditions used to simulate $C_R(L)H$ and $C_E(L)H$ with the algorithm described in Appendix C.3. Specifically, I define the relevant threshold for recessions z_R such that $f(z_R)$ is equal to the share of NBER recessions in the sample.[24] Then, I define $z_{R,\tau}$ the quantile of z_t that corresponds to z_R; the threshold for expansions z_E is obtained as the value of z_t that corresponds to its $1 - z_{R,\tau}$ quantile. In other words, I look at the response of GaR risk measures during milder recession/booms. Results are reported in Figure 12. As expected, the discrepancy between responses during slowdowns and booms is lower than in the baseline results, but interpretations and conclusions remain unaltered.

Fourth, instead of estimating the smoothness parameter ϕ as described in Section 2, I calibrate it to match the share of NBER recession in the considered sample, as in Auerbach and Gorodnichenko (2012). Results quantitatively very similar.

Finally, I test the robustness of results against two minor modelling variations. In particular, I change the number of lags in the VAR (hence, quantile predictors) and the length of the moving average used to compute the state indicator z_t. It turns out that these variations do not affect the qualitative conclusions of the paper.

[24] This is the definition I use to calibrate the smoothness parameter of the transition function, as described in Section 2.

5 Concluding remarks

Recent years have witnessed an increasing interest of monetary policy-makers towards macroeconomic downside risk. However, despite a growing attention, evidence on the relation between monetary policy and such risk is still scarce. This paper aims to fill this gap. In particular, I analyse the causal link between monetary interventions and a specific set of downside risk measures. I find that monetary policy is able to drive downside risk and that this ability is much more pronounced during economic slowdowns. The discrepancy can be explained by the asymmetric response to monetary interventions of financial indicators, which in turn contribute in explaining the state-dependent response of Growth-at-Risk, which ultimately determines the response of all downside risk measures. I obtain these results estimating newly proposed state-dependent quantile IRFs.

References

Adrian, T., Boyarchenko, N. and Giannone, D. (2019), 'Vulnerable growth', *American Economic Review* **109**(4), 1263–89.

Adrian, T., Duarte, F., Liang, N. and Zabczyk, P. (2020), Nkv: A new keynesian model with vulnerability, *in* 'AEA Papers and Proceedings', Vol. 110, American Economic Association 2014 Broadway, Suite 305, Nashville, TN 37203, pp. 470–476.

Alpanda, S., Granziera, E. and Zubairy, S. (2021), 'State dependence of monetary policy across business, credit and interest rate cycles', *European Economic Review* **140**, 103936.

Auerbach, A. J. and Gorodnichenko, Y. (2012), 'Measuring the output responses to fiscal policy', *American Economic Journal: Economic Policy* **4**(2), 1–27.

BoE (2020), 'Monetary policy report'.

Bruce, E. (1997), 'Inference in tar models', *Nonlinear Dynamics and Econometrics* **1**, 119–131.

Bruns, M. and Piffer, M. (2023), 'Tractable bayesian estimation of smooth transition vector autoregressive models', *The Econometrics Journal* .

Caggiano, G., Castelnuovo, E. and Nodari, G. (2022), 'Uncertainty and monetary policy in good and bad times: A replication of the vector autoregressive investigation by bloom (2009)', *Journal of Applied Econometrics* **37**(1), 210–217.

Caggiano, G., Castelnuovo, E. and Pellegrino, G. (2017), 'Estimating the real effects of uncertainty shocks at the zero lower bound', *European Economic Review* **100**, 257–272.

Caldara, D., Cascaldi-Garcia, D., Cuba-Borda, P. and Loria, F. (2021), 'Understanding growth-at-risk: A markov switching approach', *Available at SSRN 3992793* .

Chavleishvili, S., Engle, R. F., Fahr, S., Kremer, M., Manganelli, S. and Schwaab, B. (2021), 'The risk management approach to macro-prudential policy'.

Cho, D. and Rho, S. (2023), 'Reassessing growth vulnerability', *Journal of Applied Econometrics* .

Clark, T. E., Huber, F., Koop, G., Marcellino, M. and Pfarrhofer, M. (2024), 'Investigating growth-at-risk using a multicountry non-parametric quantile factor model', *Journal of Business & Economic Statistics* (just-accepted), 1–22.

Debortoli, D., Forni, M., Gambetti, L. and Sala, L. (2023), Asymmetric monetary policy tradeoffs, Technical report.

Degasperi, R. and Ricco, G. (2021), Information and policy shocks in monetary surprises, Technical report, Working Paper.

Delle Monache, D., De Polis, A. and Petrella, I. (2023), 'Modeling and forecasting macroeconomic downside risk', *Journal of Business & Economic Statistics* pp. 1–27.

ECB (2024), 'Monetary policy statement'.

FED (2008), 'Monetary policy report to the congress'.

Forni, M., Gambetti, L., Maffei-Faccioli, N. and Sala, L. (2023), 'The impact of financial shocks on the forecast distribution of output and inflation'.

Forni, M., Gambetti, L. and Ricco, G. (2022), 'External instrument svar analysis for non-invertible shocks'.

Forni, M., Gambetti, L. and Sala, L. (2024), 'Downside and upside uncertainty shocks', *Journal of the European Economic Association* p. jvae024.

Garcia, R. and Schaller, H. (2002), 'Are the effects of monetary policy asymmetric?', *Economic inquiry* **40**(1), 102–119.

Gertler, M. and Karadi, P. (2015), 'Monetary policy surprises, credit costs, and economic activity', *American Economic Journal: Macroeconomics* **7**(1), 44–76.

Gonçalves, S., Herrera, A. M., Kilian, L. and Pesavento, E. (2023), 'State-dependent local projections'.

Iseringhausen, M., Petrella, I. and Theodoridis, K. (2023), 'Aggregate skewness and the business cycle', *Review of Economics and Statistics* pp. 1–37.

Jordà, Ò., Schularick, M. and Taylor, A. M. (2020), 'The effects of quasi-random monetary experiments', *Journal of Monetary Economics* **112**, 22–40.

Kelley, T. L. (1947), *Fundamentals of statistics*, number 2, Harvard University Press.

Koenker, R. and Bassett Jr, G. (1978), 'Regression quantiles', *Econometrica: journal of the Econometric Society* pp. 33–50.

Koop, G., Pesaran, M. H. and Potter, S. M. (1996), 'Impulse response analysis in nonlinear multivariate models', *Journal of econometrics* **74**(1), 119–147.

Lanne, M. and Nyberg, H. (2016), 'Generalized forecast error variance decomposition for linear and nonlinear multivariate models', *Oxford Bulletin of Economics and Statistics* **78**(4), 595–603.

Lerman, P. (1980), 'Fitting segmented regression models by grid search', *Journal of the Royal Statistical Society Series C: Applied Statistics* **29**(1), 77–84.

Lo, M. C. and Piger, J. (2005), 'Is the response of output to monetary policy asymmetric? evidence from a regime-switching coefficients model', *Journal of Money, credit and Banking* pp. 865–886.

Loria, F., Matthes, C. and Zhang, D. (2022), 'Assessing macroeconomic tail risk', *Available at SSRN 4002665* .

Miranda-Agrippino, S. and Ricco, G. (2021), 'The transmission of monetary policy shocks', *American Economic Journal: Macroeconomics* **13**(3), 74–107.

Peersman, G. and Smets, F. (2001), 'Are the effects of monetary policy in the euro area greater in recessions than in booms?', *Available at SSRN 356041* .

Plagborg-Møller, M., Reichlin, L., Ricco, G. and Hasenzagl, T. (2020), 'When is growth at risk?', *Brookings Papers on Economic Activity* **2020**(1), 167–229.

Romer, C. D. and Romer, D. H. (2004), 'A new measure of monetary shocks: Derivation and implications', *American economic review* **94**(4), 1055–1084.

Tenreyro, S. and Thwaites, G. (2016), 'Pushing on a string: Us monetary policy is less powerful in recessions', *American Economic Journal: Macroeconomics* **8**(4), 43–74.

Wolf, E. (2021), 'Estimating growth at risk with skewed stochastic volatility models', *Available at SSRN 4030094* .

A Figures

Figure 5: Transition function

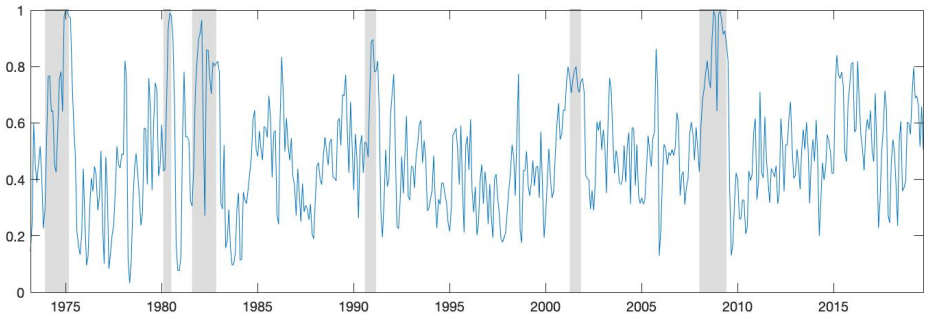

This figure plots the transition function $f(z_t)$, where z_t is a standardized 2-months backward-looking industrial production growth moving average and $\phi = 2.06$. Vertical shaded bands represents NBER recessions.

Figure 6: Conditional (on ϕ) QR-VAR Loss function

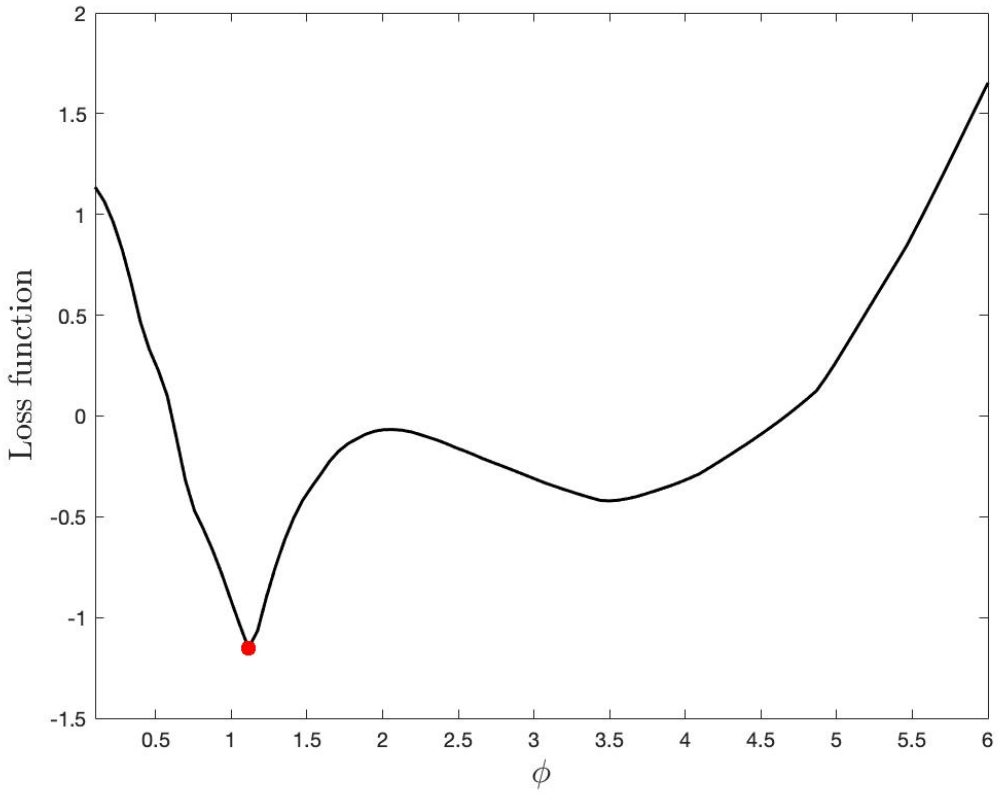

This figure plots of the loss function defined in Equation 13, evaluated at each discrete value of ϕ contained in Φ. The red dot denotes the minimum value assumed by the function (i.e., when evaluated in ϕ^*).

Figure 7: Predicted quantiles

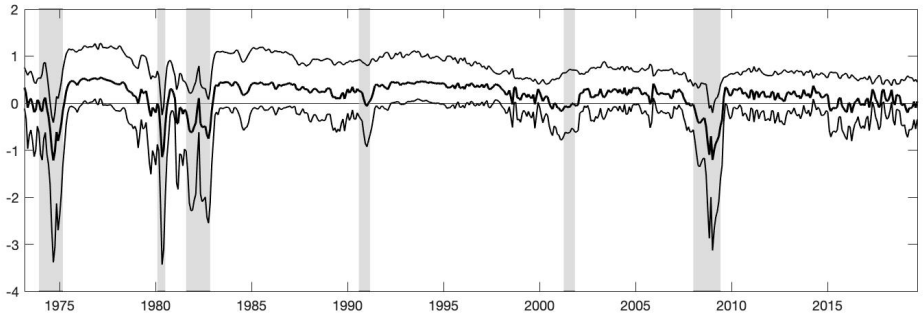

This figure plots the 95^{th}, 50^{th} and 5^{th} estimated quantiles of the forecast density of output growth.

Figure 8: GIRFs - STVAR variables

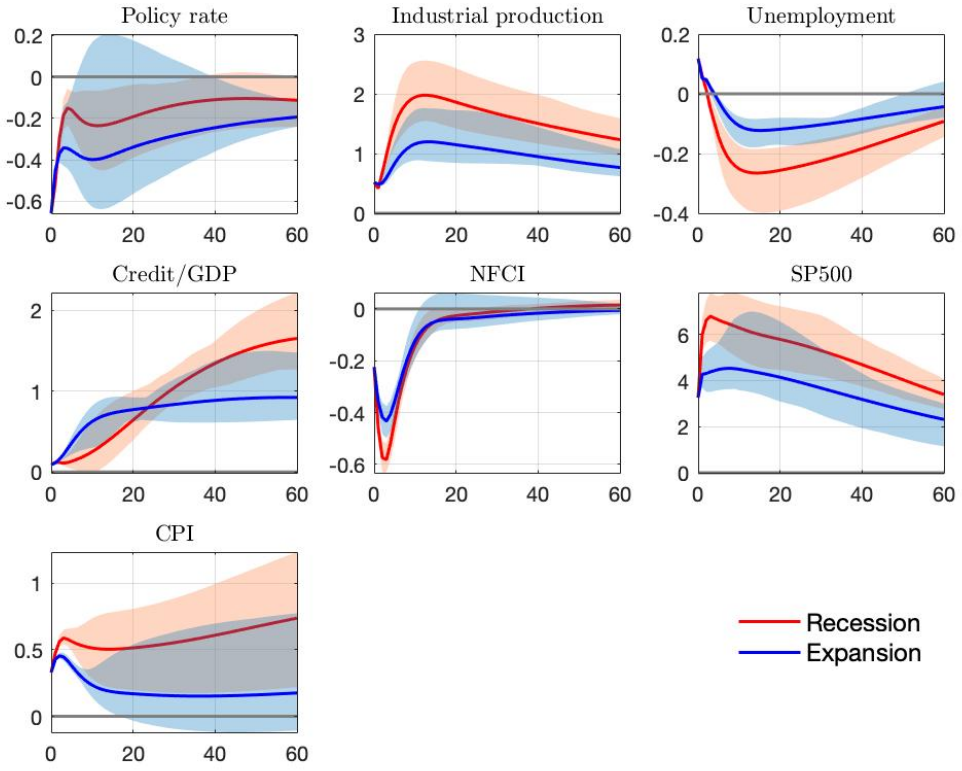

This figure plots generalized IRFs in recession (red) and expansion (blue). Confidence bands are reported at the 68% level. The size of the shock is calibrated to generate an average decrease of 50 basis points in the policy rate on impact in each state.

Figure 9: Quantiles - Impulse Response Functions

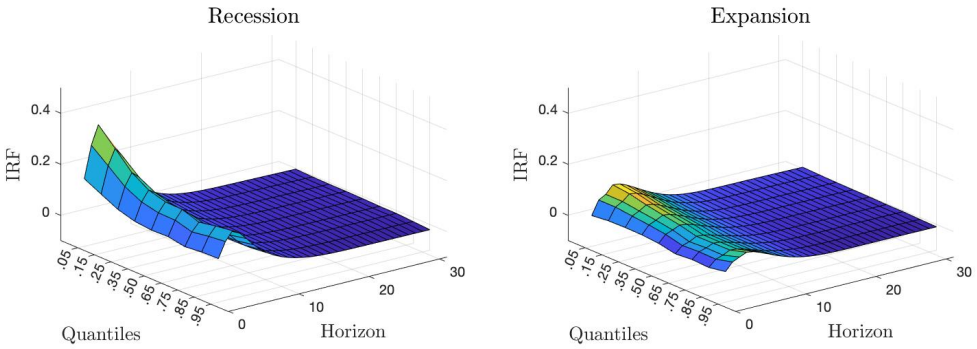

This figure plots representative quantile IRFs to an expansionary monetary policy shock, conditional on the monetary intervention occurring in recession or expansion.

Figure 10: Robustness 1 - $\beta'_{\tau,s}(L)$

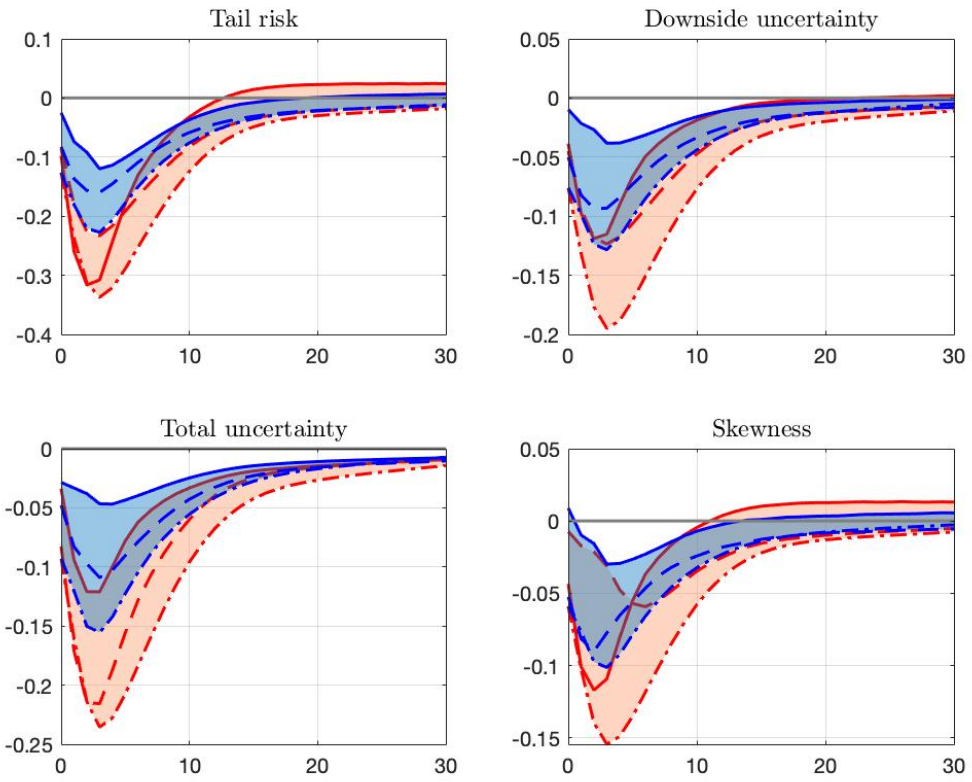

Solid lines are computed using $\tau = \{0.1, 0.9\}$ in place of $\tau = \{0.05, 0.95\}$ to represent the left and the right tails of the forecast density, respectively; dashed lines represent responses of moments of a 6-months ahead forecast distribution; dash-dotted lines are obtained using a linear quantile forecasting model (i.e., imposing $\beta'_{\tau,R}(L) = \beta'_{\tau,E}(L)$). Shaded bands are simply used to visualize the area spanned by the different models, roughly describing "modelling uncertainty". Red (blue) lines represents recessionary (expansionary) periods.

Figure 11: Robustness 2 - W

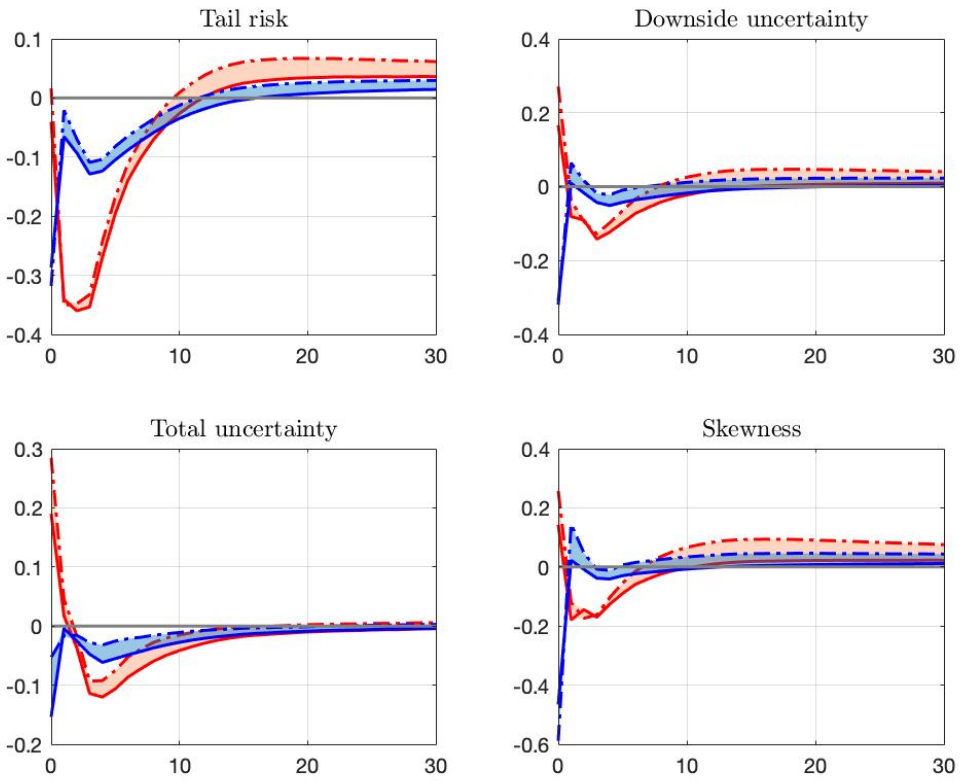

Solid lines represent responses obtained including in ST-QRs only regressors whose associated coefficient is significant at 5% in at least one of the the linear quantile regressions for $\tau = \{0.05, 0.5, 0.95\}$. Dashed-dotted lines are computed setting the matrix W to be an identity. Shaded bands are simply used to visualize the area spanned by the different models, roughly describing "modelling uncertainty". Red (blue) lines represents recessionary (expansionary) periods.

Figure 12: Robustness 3 - Mild recession/booms

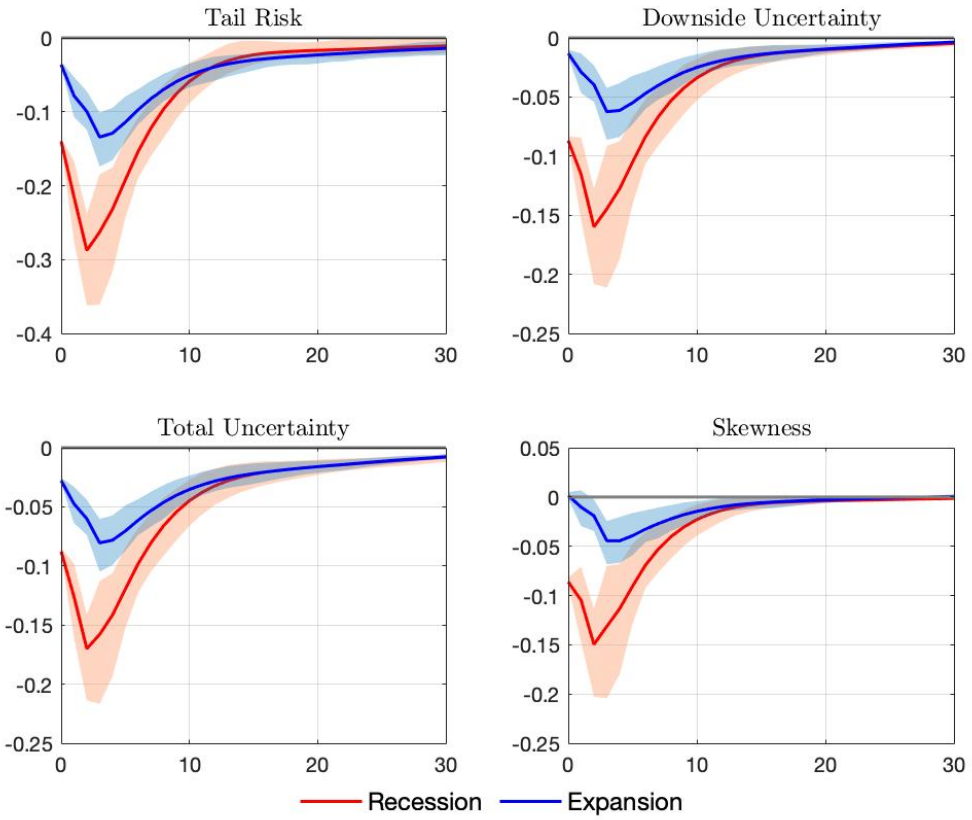

This Figure plots the response of GaR risk measures to an expansionary monetary policy shock. The parameters defining the expansion and recession sets are less stringent, comapred to the baseline case.

B Tables

Table 3: Downside risk measures - Correlations

	Tail risk	Downside uncertainty	Total uncertainty	Skewness
Tail risk	.	.	.	.
Downside uncertainty	0.94	.	.	.
Total uncertainty	0.90	0.95	.	.
Skewness	0.80	0.86	0.68	.

This table shows the correlation among estimated GaR risk measures.

Table 4: GFEVD - STVAR variables

	$h = 0$		$h = 12$		$h = 24$	
	Recession	Expansion	Recession	Expansion	Recession	Expansion
Policy rate	16.10	16.10	4.24	5.65	2.76	5.25
INDPRO	9.28	9.28	41.39	14.06	45.77	17.56
UNEMP	1.43	1.43	19.26	2.23	22.74	3.00
NFCI	20.16	20.16	25.89	9.65	24.48	9.08
SP500	9.07	9.07	17.29	7.80	14.17	6.39
CPI	17.91	17.91	15.24	6.39	10.14	2.58
Commodity	45.79	45.79	51.62	23.06	46.03	13.48

This table shows the the variance of variables of interest explained by the monetary policy shock at different forecast horizons, across economic states.

Table 5: Quantile regression - All regressors

	$\tau = 0.05$			$\tau = 0.5$			$\tau = 0.95$		
	Rec	Exp	Lin	Rec	Exp	Lin	Rec	Exp	Lin
Policy rate	0.22	-0.26	-0.01	0.11	0.11	0.24***	0.23	-0.03	0.24***
INDPRO	-0.24	0.13	0.10*	0.06	-0.05	0.04	0.03	0.25	0.04
UNEMP	-0.25	0.02	0.00	-0.39	0.14	0.03	-0.16	0.10	0.03
NFCI	-0.99	-0.55	-0.49***	-0.43	0.06	-0.45***	-0.66	-0.01	-0.45***
SP500	0.01	0.00	0.02*	0.04	0.01	0.01	0.03	0.01	0.01
CPI	0.21	0.01	0.04	-0.05	-0.13	-0.03	0.36	0.17	-0.03
Commodity	-0.06	0.01	0.05	0.14	0.11	0.18***	0.07	0.03	0.18***
(lag) Policy rate	-0.03	0.33	0.12**	-0.08	-0.07	-0.18***	-0.19	0.12	-0.18***
(lag) INDPRO	0.22	-0.12	-0.10**	-0.05	0.04	-0.05	-0.01	-0.26	-0.05
(lag) UNEMP	0.60	0.10	0.20	0.49	-0.04	0.09	0.40	-0.01	0.09
(lag) NFCI	0.21	0.31	-0.12	0.12	-0.23	0.21***	0.28	-0.19	0.21***
(lag) SP500	0.00	0.01	-0.01	-0.04	0.00	0.00	-0.02	-0.01	0.00
(lag) CPI	-0.19	0.02	-0.02	0.06	0.11	0.03	-0.36	-0.15	0.03
(lag) Commodity	0.05	-0.07	-0.08	-0.16	-0.10	-0.19***	-0.10	-0.05	-0.19***

*This table reports estimated quantile regression coefficients. It shows estimates relative to relevant quantiles, across states. Note that ***, **, * denote significance of estimates at the 1%, 5% and 10% levels.*

Table 6: Quantile regression - Selected regressors

	$\tau = 0.05$		$\tau = 0.5$		$\tau = 0.95$	
	Recession	Expansion	Recession	Expansion	Recession	Expansion
NFCI	-0.82	-0.12	-0.35	-0.13	-0.35	-0.09
SP500	0.00	0.00	0.00	0.00	0.00	0.00
(lag) Policy rate	0.04	0.02	-0.01	0.00	0.00	0.00

This table reports estimated quantile regression coefficients, after the selection of relevant regressors.

C Extensions and Algorithms

C.1 Shaping the forecast density

In this section, I extend the model described in Section 2 imposing *ex post* distributional assumptions. The objective of this exercise is to relate directly my work to that of Adrian et al. (2019), who recover the exact shape of the forecast density of output growth semi-parametrically.

First, I reproduce the main findings of the seminal paper. Specifically, I fit quantiles predicted using Equation 5 into skewed-t distributions.[25] More in detail, I cluster predicted quantiles in "recession" and "expansion" sets based on whether the time of the prediction for such quantiles is classified as NBER recession. Then, I consider the average predicted quantiles of each of these two sets and fit them into skewed-t distributions. The densities that I obtain are plotted in Figure 13 with continuous lines. Overall results confirm the main conclusions of Adrian et al. (2019): predicted densities in recessions are more dispersed, left-skewed and shifted to the left compared to densities in normal times.

Second, I recover the shape of the predicted density in the aftermaths of an expansionary monetary policy shock, across states. In order to obtain post-shock predicted quantiles, I simply sum baseline predicted quantiles in expansion/recession (obtained as described above) with the corresponding state QIRF; then, I fit the obtained quantiles into skewed-t distribution as in Adrian et al. (2019). In Figure 13, I plot the densities across states one quarter after the shock (i.e., the peak response horizon) with dotted lines.

Figure 13: Densities before and after a monetary policy shock

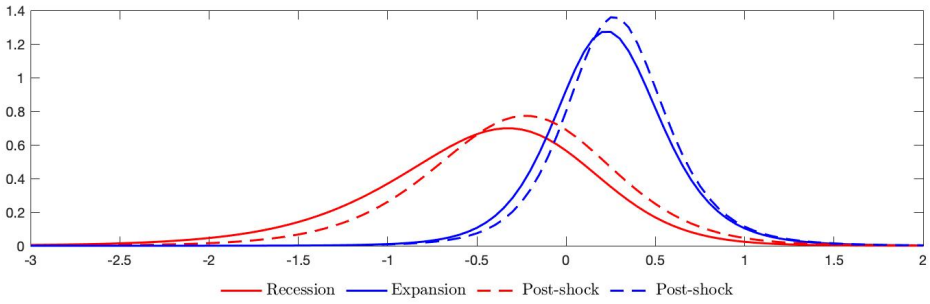

This figure plots predicted densities of output growth before and after an expansionary monetary policy shock, distinguishing between expansions and recessions.

Results essentially confirm what highlighted in previous sections. An expansionary monetary policy shock shifts to the right the forecast density of output growth, decrease its dispersion and left-skewness mainly because of variations in the left tail. The effects are more pronounced if the monetary intervention occurs during an economic slowdown.

[25] The main difference between Adrian et al. (2019) model and mine is that I use smooth-transition quantile regressions instead of linear quantile regressions to predict quantiles of interest.

This results closely speak to those of Adrian et al. (2019). Specifically, the reference paper shows that the forecast density of output growth becomes more dispersed and left-skewed during recessions; I show that a significant component of such dynamics could be explained by monetary policy operations during slowdowns.

C.2 Identification of shocks with external instrument

In this section, I briefly describe how I identify the relevant column of the impact matrix H thanks to information coming from an external instrument, following the procedure of Gertler and Karadi (2015). Specifically, I assume that an observed instrument ι exists such that the following conditions hold

$$\begin{aligned} &\mathbb{E}[\iota_t \zeta_{1,t}] = \alpha \neq 0 \\ &\mathbb{E}[\iota_t \zeta_{n,t}] = 0 \qquad\qquad n = 2, ..., N \end{aligned} \tag{15}$$

where ι_t is the instrument, $\zeta_{1,t}$ is the structural shock of interest, $\zeta_{n,t}$ is any of the remaining structural shocks.[26] I also assume that the shocks are fundamental. Given the assumptions, the following holds

$$H_{1,1} = \gamma_1 \omega \tag{16}$$

and

$$H_{n,1} = \gamma_n H_{1,1} \tag{17}$$

where $H_{1,1}$ is the first entry of the first column of the impact matrix H; similarly, $H_{n,1}$ is the n^{th} entry of the first column; $\omega = var[\iota_t]/\alpha$; γ_1 is the coefficient obtained regressing the reduced-form residuals associated to the policy indicator on the instrument; γ_n is obtained regressing reduced-form residuals associated to the n^{th} endogenous variable in y_t on fitted reduced-form residuals obtained using γ_1 and ι. Finally, exploiting the fact that $\Sigma = HH'$, the object $H_{1,1}$ can be recovered following Gertler and Karadi (2015) as

$$H_{1,1} = [\sigma - (\tilde{\sigma} - \sigma\gamma)'[\sigma\gamma\gamma' - (\tilde{\sigma}\gamma' + \gamma\tilde{\sigma}') + \tilde{\Sigma}]^{-1}(\tilde{\sigma} - \sigma\gamma)]^{\frac{1}{2}} \tag{18}$$

where $\gamma = \begin{bmatrix}\gamma_2 & ... & \gamma_N\end{bmatrix}'$, $\sigma = \Sigma_{1,1}$ and $\tilde{\sigma} = \Sigma_{2:N,1}$ and $\tilde{\Sigma} = \Sigma_{2:N,2:N}$. This allows to recover the absolute identifying column $H_{.,1}$, and in turn the full impact matrix.[27]

The main limitation of this approach is that it does not consent to have state-dependence in the impact matrix and, as a consequence, non-linearity only comes from the reduced-form coefficients. Consequently, asymmetries across states generated within the framework just described should be thought as a lower bound of non-linearity.[28]

[26] The order of shocks in ζ_t is irrelevant, so there is no loss of generality in assuming the structural shock of interest to be ordered first.

[27] The full impact matrix can be recovered finding an orthonormal matrix U, such that $(chol(\Sigma)U)_1 = H_{.,1}$. Note that the full matrix is not needed for identification purposes, but only to compute variance decompositions.

[28] State-dependent impact matrices could be recovered from state-dependent residuals covariance matrices. However, as mentioned above, obtaining such covariances would require distributional assumptions to define proper likelihood functions. As I opt to avoid assumptions to leave quantiles dynamics unconstrained, I rely on a linear impact matrix to identify shocks.

C.3 Generalized Quantile Impulse Response Functions (GQIRFs)

A GIRF is broadly defined as a difference between two conditional expectations with a different conditioning set. Specifically, one set includes the realization of a shock, whereas the other does not. More formally, I follow Koop et al. (1996) and Caggiano et al. (2022) to define a GIRF as

$$GIRF(h, \delta, \lambda) = \mathbb{E}[y_{t+h}|\delta, \lambda] - \mathbb{E}[y_{t+h}|\lambda] \tag{C.2.1}$$

where y_t is defined as in Equation 6, h is the horizon of the GIRF and δ is the shock. I distinguish between GIRFs across states by conditioning on the initial condition λ, which defines the regime in place when the shock δ hits. Wheres standard IRFs are computed conditional on a state, this definition of impulse responses allows to condition on an initial condition only (allowing the state to be different at different horizons). The simulation algorithm used to compute GIRFs in this paper is reported below.

1. Estimate relevant objects
   (a) estimate the ST-VAR to obtain $\{\xi_t, \Sigma, B_R(L), B_E(L)\}$;
   (b) apply the 2SLS procedure to obtain $\{\gamma\}$;
   (c) obtain the identifying matrix H as described in Section 2
   (d) estimate ST-QR to obtain $\{\beta_R^\tau, \beta_E^\tau\}$
2. Construct histories (i.e., initial conditions)

$$\lambda_t = \begin{bmatrix} y_t & y_{t-1} & ... & y_{t-m-1} \end{bmatrix}$$

   where m is the length of the moving average window used to compute the transition variable z_t.
3. Cluster histories into expansion and recession sets
   (a) compute transition variable z_{λ_t} for each history λ_t
   (b) compare z_{λ_t} to a cut-off values z_R and z_E
   (c) assign λ_t to the set Λ_E if $z_{\lambda_t} > z_E$ and to Λ_R if $z_{\lambda_t} < z_R$

   The cut-off values z_R and z_E are chosen such that 1% of histories belong to Λ_R and 1% to Λ_E
4. Select randomly, with replacement, $\mathcal{I}$ histories from the relevant set (Λ^R to build GQIRF in recession, Λ^E for expansion)
5. For each of the history draw i
   (a) compute structural shocks from ST-VAR matrix of residuals ξ (obtained stacking residuals over time, horizontally; dimension NxT)

$$\zeta = H^{-1}\xi$$

(b) draw with replacement columns from ζ to obtain $\mathcal{J}$ matrices of bootstrapped structural shocks of size NxH (where N is the number of variables in the VAR and H is the horizon of the GIRF), the j^{th} matrix being defined as ζ_i^j

(c) For each of the $\mathcal{J}$ matrices

i. perturbate the k^{th} element of the first column of ζ_i^j by an amount δ, where k is the position of the shock of interest in the vector of structural shocks; define the new obtained matrix $\zeta_i^{j,\delta}$

ii. transform the two matrices of structural shocks back into matrices of reduced-form residuals

$$\xi_i^j = H\zeta_i^j$$
$$\xi_i^{j,\delta} = H\zeta_i^{j,\delta}$$

iii. simulate the evolution of y_t (i.e., first column of the drawn λ) over t up to h using the STVAR coefficients

$$y_t = (f(z_{t-1})B_R(L) + (1 - f(z_{t-1}))B_E(L))y_t + \xi_{i,t}^j$$

where $z_0 = z_{\lambda_i}$. At each iteration over t, simulate the evolution of quantiles using the estimated coefficient in the ST-QRs

$$x_t^\tau = (f(z_{t-1})\beta_{\tau,R}(L)' + (1 - f(z_{t-1}))\beta_{\tau,E}(L)')Wy_t$$

Update the value of z_{t-1} at each iteration over t, based on the simulated values of y_t (to account for endogenous state transition). Obtain the h-steps ahead simulation, $x_{i,t+h}^{\tau,j}$. Perform the same operations, substituting $\xi_{i,t}^j$ with $\xi_{i,t}^{j,\delta}$, and obtain the simulated values given the shock, $x_{i,t+h}^{\tau,j,\delta}$

iv. compute conditional GQIRF as

$$GQIRF(h, \delta, \lambda_i)^j = x_{i,t+h}^{\tau,j,\delta} - x_{i,t+h}^{\tau,j}$$

(d) average over all bootstrapped residuals j

$$GQIRF(h, \delta, \lambda_i) = \mathcal{J}^{-1} \sum_{j=1}^{\mathcal{J}} GQIRF(h, \delta, \lambda_i)^j$$

(e) average over all histories i

$$GQIRF(h, \delta) = \mathcal{I}^{-1} \sum_{i=1}^{\mathcal{I}} GQIRF(h, \delta, \lambda_i)$$

Note that the GQIRFs obtained applying the algorithm described above are dependent on the sign and the size of the perturbation δ.

C.4 Generalized Forecast Error Variance Decomposition

The Generalized Forecast Error Variance Decomposition (GFEVD) of interest, defined as the variation in y_k due to shock δ_j as a share of total variation at horizon $\tilde{h}$, conditional on history λ_i, reads

$$GFEVD_{kj}^{\tilde{h}}(\delta_j) = \mathcal{I}^{-1} \sum_{i=1}^{\mathcal{I}} \frac{\sum_{h=0}^{\tilde{h}} GIRF_k(h, \delta_j, \lambda_i)^2}{\sum_{j=1}^{N} \sum_{h=0}^{\tilde{h}} GIRF_k(h, \delta_j, \lambda_i)^2} \tag{C.3.1}$$

where $GIRF_k(h, \delta_j, \lambda_i)$ is computed as described in step 5 in Appendix C.3. Note that GIRFs are computed conditional on the size and the sign of the shocks $\Delta = (\delta_1, ..., \delta_N)$, a condition that is inherited by the GFEVD. In order to ensure comparability across shocks-responses, I set $\Delta = (\bar{c}, ..., \bar{c})$, where $\bar{c}$ is an arbitrary constant.